

Collaboration-Aware Graph Convolutional Networks for Recommendation Systems

Yu Wang

yu.wang.1@vanderbilt.edu
Vanderbilt University

Yi Zhang

yi.zhang@vanderbilt.edu
Vanderbilt University

ABSTRACT

By virtue of the message-passing that implicitly injects collaborative effect into the embedding process, Graph Neural Networks (GNNs) have been successfully adopted in recommendation systems (e.g., LightGCN, GTN, and UltraGCN). Nevertheless, most of existing message-passing mechanisms in recommendation are directly inherited from GNNs without any recommendation-tailored modification. Although some efforts have been made towards simplifying GNNs to improve the performance/efficiency of recommendation, no study has comprehensively scrutinized how message-passing captures collaborative effect and whether the captured effect would benefit the prediction of user preferences over items.

Therefore, in this work we aim to demystify the collaborative effect captured by message-passing in GNNs and develop new insights towards customizing message-passing for recommendation. First, we theoretically analyze how message-passing captures and leverages the collaborative effect in predicting user preferences. Then, to determine whether the captured collaborative effect would benefit the prediction of user preferences, we propose a recommendation-oriented topological metric, Common Interacted Ratio (CIR), which measures the level of interaction between a specific neighbor of a node with the rest of its neighborhood set. Inspired by our theoretical and empirical analysis, we propose a recommendation-tailored GNN, Augmented Collaboration-Aware Graph Convolutional Network (CAGCN*), that extends upon the LightGCN framework and is able to selectively pass information of neighbors based on their CIR via the Collaboration-Aware Graph Convolution. Experimental results on six benchmark datasets show that CAGCN* outperforms the most representative GNN-based recommendation model, LightGCN, by 9% in Recall@20 and also achieves more than 79% speedup. Our code is publicly available at <https://github.com/YuWVandy/CAGCN>

CCS CONCEPTS

- Information systems → Data mining.

Permission to make digital or hard copies of all or part of this work for personal or classroom use is granted without fee provided that copies are not made or distributed for profit or commercial advantage and that copies bear this notice and the full citation on the first page. Copyrights for components of this work owned by others than ACM must be honored. Abstracting with credit is permitted. To copy otherwise, or republish, to post on servers or to redistribute to lists, requires prior specific permission and/or a fee. Request permissions from permissions@acm.org.

Conference acronym 'XX, June 03–05, 2018, Woodstock, NY

© 2018 Association for Computing Machinery.

ACM ISBN 978-1-4503-XXXX-X/18/06...\$15.00

<https://doi.org/XXXXXX.XXXXXXX>

Yuying Zhao

yuying.zhao@vanderbilt.edu
Vanderbilt University

Tyler Derr

derr.tyler@vanderbilt.edu
Vanderbilt University

KEYWORDS

recommendation systems, graph neural networks, collaborative effect, common interacted ratio

ACM Reference Format:

Yu Wang, Yuying Zhao, Yi Zhang, and Tyler Derr. 2018. Collaboration-Aware Graph Convolutional Networks for Recommendation Systems. In *Woodstock '18: ACM Symposium on Neural Gaze Detection, June 03–05, 2018, Woodstock, NY*. ACM, New York, NY, USA, 13 pages. <https://doi.org/XXXXXX.XXXXXXX>

1 INTRODUCTION

Nowadays, to alleviate information overload through helping users discover items of interest [4, 41], personalized recommendation has been widely deployed in real-world applications such as social media, advertising, and e-commerce. Given historical user-item interactions (e.g. click, purchase, review, and rate), the key of recommendation systems is to leverage the Collaborative Effect [5, 13, 30] to predict how likely users will interact with items. A common paradigm for modeling collaborative effect is to first learn embeddings of users/items capable of recovering historical user-item interactions and then perform top-k recommendation based on the pairwise similarity between the learned user/item embeddings.

Since historical user-item interactions can be naturally represented as a bipartite graph with users/items being nodes and interactions being edges [11, 18, 30] and given the unprecedented success of GNNs in node representation learning [14, 15, 33], recent research has started to leverage GNNs to learn user/item embeddings for recommendation. Two pioneering work NGCF [30] and LightGCN [11] leverage graph convolution to aggregate messages from local neighborhoods, which directly injects the collaborative signal into user/item embeddings. Close on the heels of the successful adoption of graph convolution to capture collaborative signals, more recent work [1, 37] explore the robustness and self-supervised learning of graph convolution for recommendation. However, the message-passing mechanisms in all previous recommendation models are directly inherited from GNNs without carefully justifying how it captures collaborative signals and whether the captured collaborative signals would benefit the prediction of user preferences over items. Such ambiguous understanding on how the message-passing captures collaborative signals would pose the risk of learning uninformative or even harmful user/item representations when adopting GNNs in recommendation. For example, [6] shows that a large portion of user interactions cannot reflect their actual purchasing behaviors. In this case, blindly passing messages following

existing styles of GNNs could capture harmful collaborative signals from these unreliable interactions, which corrupts user/item embeddings and then hinders GNN-based model performance.

To avoid collecting noisy or even harmful collaborative signals captured by message-passing in traditional GNNs, existing work GTN [6] proposes to adaptively propagate user/item embeddings by adjusting the weight of edges based on items' similarity to users' main preferences (i.e., the trend). However, such similarity is still computed based on the learned embeddings that implicitly encode noisy collaborative signals from unreliable user-item interactions. Worse still, calculating edge weights based on user/item embeddings along the training on the fly is computationally prohibitive and hence prevents the model from being deployed in industrial-level recommendations. UltraGCN [20] directly approximates message-passing by optimizing the link prediction loss derived from infinite-layer propagation, which seemingly avoids propagation along unreliable interactions but actually squeezes noisy collaborative signals unconsciously into user/item embeddings through optimizing embeddings over unreliable interactions.

Despite the fundamental importance of capturing beneficial collaborative signals by message-passing, the related studies are still in their infancy. To fill this crucial gap, we aim to demystify the collaborative effect captured by message-passing in GNNs and develop new insights towards customizing message-passing for recommendations. Furthermore, these insights motivate us to design a class of recommendation-tailored GNNs, namely Collaboration-Aware Graph Convolutional Network (CAGCN) and its augmented version (CAGCN*), that extend upon the LightGCN framework and are able to selectively pass information of neighbors based on their CIR via the Collaboration-Aware Graph Convolution. Note that in the following, we use CAGCN(*) to refer to these two models together. Our major contributions are summarized as follows:

- **Novel Perspective on Collaborative Effect:** We demystify the collaborative effect captured by message-passing in GNNs by theoretically analyzing how message-passing helps users leverage collaborative signals and when such collaborative signals are beneficial in computing users' ranking over items.
- **Novel Recommendation-tailored Topological Metric:** We then propose a recommendation-oriented topological metric, Common Interacted Ratio (CIR), and further empirically demonstrate the capability of CIR to quantify the benefits of aggregating messages from neighborhoods.
- **Novel Recommendation-tailored Graph Convolution:** We incorporate CIR into message-passing and ultimately propose a novel class of Collaboration-Aware Graph Convolutional Networks. Then we prove that CAGCN* can go beyond 1-WL test, and demonstrate its superiority via comprehensive experiments on real-world datasets including two newly collected/introduced datasets and provide an in-depth interpretation on its advantages.

Next, Section 2 introduces preliminaries. In Section 3, we analyze how message-passing captures collaborative effect and further propose CIR to measure whether the captured collaborative effect would benefit the prediction of user preference. Following that, we introduce CAGCN(*) in Section 4 and evaluate it by performing extensive experiments in Section 5. Related work is presented in Section 6. Finally, we conclude and discuss future work in Section 7.

2 PRELIMINARY AND TASK OVERVIEW

Here we introduce notations used in this work and briefly review GNN-based models for recommendation, which paves the way to demystify the collaborative effects captured by message-passing.

We summarize all notations used throughout this paper in Table 6 in Appendix D. Let $\mathcal{G} = (\mathcal{V}, \mathcal{E})$ be the user-item bipartite graph, where the node set $\mathcal{V} = \mathcal{U} \cup \mathcal{I}$ includes the user set \mathcal{U} with n user nodes and the item set \mathcal{I} with m item nodes. Following previous work [11, 20, 30], we only consider the implicit user-item interactions and denote them as edges $\mathcal{E} = \{e_1, \dots, e_{|\mathcal{E}|}\}$ where e_{pq} represents the edge between node p and q . The network topology is described by its adjacency matrix $\mathbf{A} \in \{0, 1\}^{(n+m) \times (n+m)}$, where $\mathbf{A}_{pq} = 1$ when $e_{pq} \in \mathcal{E}$, and $\mathbf{A}_{pq} = 0$ otherwise. The set of observed l -hops away neighbors of p is noted as \mathcal{N}_p^l , which includes all nodes whose shortest path to p is of length l based on observed user-item interactions in training set. More specifically, we let $\tilde{\mathcal{N}}_p^1 = \mathcal{N}_p^1 \cup \{p\}$ denote the one-hop neighborhood set of the node p including p itself and $\hat{\mathcal{N}}_p^1$ denote the one-hop neighborhood of p that are interacted with p but are unobserved in testing set. Moreover, we let $\tilde{\mathcal{N}}_p^l = \mathcal{V}/(\tilde{\mathcal{N}}_u^1 \cup \hat{\mathcal{N}}_u^1)$. Let \mathcal{S}_u be the neighborhood subgraph induced in \mathcal{G} by $\tilde{\mathcal{N}}_u^1$ with the node set $\mathcal{V}_{\mathcal{S}_u}$ and the edge set $\mathcal{E}_{\mathcal{S}_u}$. We use \mathcal{P}_{pq}^l to denote the set of shortest paths of length l between node p and q and denote one of such paths as P_{pq}^l . Note that $P_{pq}^l = \emptyset$ means it is impossible to have the path between p and q of length l , e.g., P_{11}^1 is impossible in an acyclic graph. Furthermore, we denote the initial embeddings of user/item nodes in graph \mathcal{G} as $\mathbf{E}^0 \in \mathbb{R}^{(n+m) \times d^0}$ with d^0 as the embedding dimension. In addition, we define the cross product of two sets as $\mathcal{A} \times \mathcal{B} = \{(a, b) | a \in \mathcal{A}, b \in \mathcal{B}\}$.

A unified template of most GNN-based recommendation models first stacks L graph convolutional layers to obtain node embeddings $\{\mathbf{E}^l \in \mathbb{R}^{(n+m) \times d^l} | l \in \{1, \dots, L\}\}$ and then combines them together to form the final representation of each user and item:

$$\mathbf{E} = \text{COMB}(\{\text{TRAN}^l(\text{MP}^l(\mathbf{E}^{l-1}, \mathbf{A}))\}, l \in \{1, \dots, L\}) \quad (1)$$

where MP^l , TRAN^l , COMB stand respectively for neighborhood messaging passing, nonlinear feature transformation at layer l , and the final combination layer. Different GNN-based recommendation models (e.g., NGCF [30], DGCF [31], and LightGCN [11]) can be obtained under this template by configuring different COMB , TRAN^l , and MP^l . Different from the setting in node classification [14, 33], each node in our recommendation setting (also in [6, 11, 20, 30]) has no semantic features but the purely learnable embeddings. Then, adding nonlinear feature transformation brings no significant benefits on recommendation performance but exacerbates the training difficulty. Therefore, we remove the TRAN^l for simplicity and leverage LightGCN [11] as the canonical architecture to exclusively explore the collaborative effect captured by messaging passing.

Given a bipartite graph constructed from the observed user-item interactions (as shown in Figure 1(a)), LightGCN first passes messages from user/item u/i 's neighbors within l -hops to u/i by:

$$\begin{aligned} \mathbf{e}_u^{l+1} &= d_u^{-0.5} \sum_{i \in \mathcal{N}_u^l} d_i^{-0.5} \mathbf{e}_i^l \\ \mathbf{e}_i^{l+1} &= d_i^{-0.5} \sum_{u \in \mathcal{N}_i^l} d_u^{-0.5} \mathbf{e}_u^l, \quad l \in \{0, 1, \dots, L\}. \end{aligned} \quad (2)$$

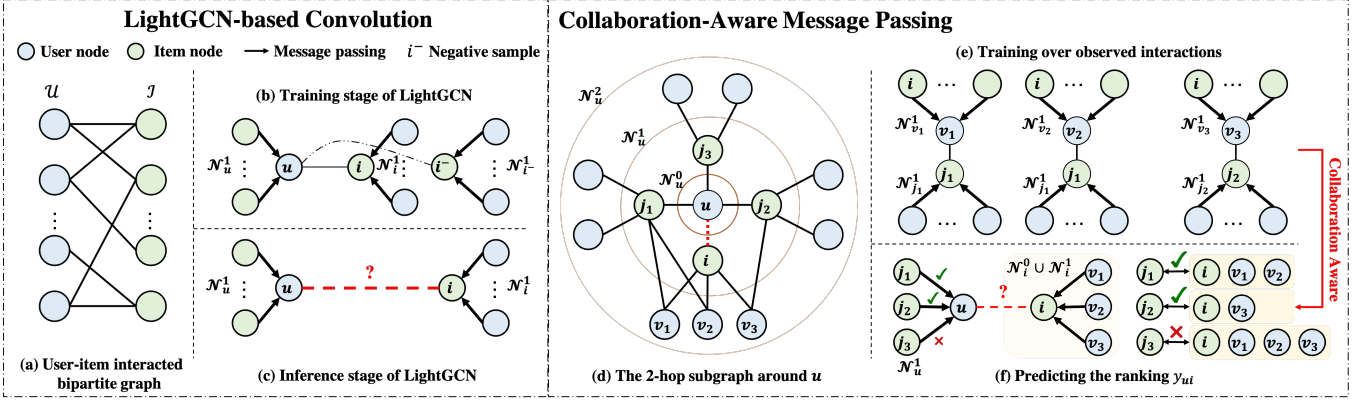


Figure 1: (a)-(c) describes the training and inference stage of LightGCN where they first pass messages from u , i , i^- 's corresponding 1-hop neighborhoods and then either optimize their embedding similarity in the training stage or compute u 's ranking over i in the inference stage. In (d)-(f), since j_1 and j_2 have more interactions with i 's neighbors than j_3 based on observed interactions, leveraging more collaborations from j_1 and j_2 than j_3 would increase u 's ranking over i , which benefits the prediction of the interaction between u and i in testing set.

Then, in the training stage, for each observed user-item interaction (u, i) , LightGCN randomly samples a negative item i^- that u has never interacted with before and obtains the triple (u, i, i^-) (as seen in Figure 1(b)), which collectively forms the set of observed training triples O . After that, the ranking scores of the user over these two items are computed as $y_{ui} = \mathbf{e}_u^\top \mathbf{e}_i$ and $y_{ui^-} = \mathbf{e}_u^\top \mathbf{e}_{i^-}$, which are finally used in optimizing the pairwise Bayesian Personalized Ranking (BPR) loss [24] and formalized as:

$$\mathcal{L}_{\text{BPR}} = \sum_{(u, i, i^-) \in O} -\ln \sigma(y_{ui} - y_{ui^-}), \quad (3)$$

where $\sigma(\cdot)$ is the Sigmoid function, and here we omit the L_2 regularization term since it is mainly for alleviating overfitting and has no influence on collaborative effect captured by message passing.

Previous works [11, 30] claim that the message-passing in Eq. (2) exploits the user-item graph by modeling higher-order connectivity and effectively injects the collaborative signal into the embedding process. However, from Figure 1(a)-(c), it is still hard to see how message-passing helps users to better capture and leverage the collaborative information from other users than the traditional Matrix Factorization (MF) models to compute users' own ranking over items. To fill this crucial gap, we round this section by raising two key questions that if solved, would help demystify the connection between message-passing and collaborative effect.

- Q_1 : How does message-passing help users leverage the collaborative effect in computing their ranking over items?
- Q_2 : When do collaborations captured by message-passing benefit the computation of users' ranking over items?

Next, we address Q_1 by theoretically deriving users' ranking over items after message-passing within the LightGCN framework and address Q_2 by proposing CIR to quantify the benefits of aggregating messages from each specific neighbor. The answers to the above two questions further motivate our design of Collaboration-Aware Graph Convolutional Networks in Section 4.

3 ANALYSIS ON THE COLLABORATIVE EFFECT IN GNN MESSAGE-PASSING

In recommendation systems, collaborative effect facilitates the prediction of a user's preference by utilizing other users' preferences or items' characteristics [25]. Therefore, to answer Q_1 , we need to seek whether we leverage other nodes' embeddings in computing a specific user's ranking over items. Following the inference procedures of LightGCN in Figure 1(c), we take the inner product between user u 's embedding and item i 's embedding after L -layer LightGCN-based message-passing to compute the ranking as¹:

$$y_{ui}^L = \left(\sum_{l_1=0}^L \sum_{j \in \mathcal{N}_u^{l_1}} \sum_{l_2=l_1}^L \beta_{l_2} \alpha_{ju}^{l_2} \mathbf{e}_j^0 \right)^\top \left(\sum_{l_1=0}^L \sum_{v \in \mathcal{N}_i^{l_1}} \sum_{l_2=l_1}^L \beta_{l_2} \alpha_{vi}^{l_2} \mathbf{e}_i^0 \right), \quad (4)$$

where $\alpha_{ju}^{l_2} = \prod_{e_{pq} \in P_{ju}^{l_2}} d_p^{-0.5} d_q^{-0.5} (\alpha_{ju}^{l_2} = 0 \text{ if } P_{ju}^{l_2} = \emptyset)$ denotes the weight of the shortest path of length l_2 from j to u , and β_{l_2} is the weight measuring contributions of propagated embeddings at layer l_2 . Specifically when $l_1 = l_2 = 0$, we have $\mathcal{N}_u^0 = \{u\}$, $\alpha_{ju}^0 = 1$, $\mathcal{N}_i^0 = \{i\}$, $\alpha_{vi}^0 = 1$. For example, we compute user u 's ranking over item i in Figure 1(c) after 1-layer message-passing following Eq (4) as:

$$y_{ui}^1 = (\beta_0 \mathbf{e}_u^0 + \beta_1 \sum_{j \in \mathcal{N}_u^1} \alpha_{ju}^1 \mathbf{e}_j^0)^\top (\beta_0 \mathbf{e}_i^0 + \beta_1 \sum_{v \in \mathcal{N}_i^1} \alpha_{vi}^1 \mathbf{e}_v^0) = \frac{\beta_0^2 \mathbf{e}_u^0 \top \mathbf{e}_i^0}{\chi(C\mathcal{E}(\mathcal{N}_u^0 \times \mathcal{N}_i^0))} + \frac{\beta_0 \beta_1 \sum_{v \in \mathcal{N}_i^1} \alpha_{vi}^1 \mathbf{e}_u^0 \top \mathbf{e}_j^0 + \beta_0 \beta_1 \sum_{j \in \mathcal{N}_u^1} \alpha_{ju}^1 \mathbf{e}_j^0 \top \mathbf{e}_i^0}{\chi(C\mathcal{E}(\mathcal{N}_u^1 \times \mathcal{N}_i^0))} + \frac{\beta_1^2 \sum_{j \in \mathcal{N}_u^1} \sum_{v \in \mathcal{N}_i^1} \alpha_{ju}^1 \alpha_{vi}^1 \mathbf{e}_j^0 \top \mathbf{e}_v^0}{\chi(C\mathcal{E}(\mathcal{N}_u^1 \times \mathcal{N}_i^1))}, \quad (5)$$

where $\chi(C\mathcal{E}(\mathcal{N}_u^{l_1} \times \mathcal{N}_i^{l_2})) = \chi(\{C\mathcal{E}(j, v) | j \in \mathcal{N}_u^{l_1}, v \in \mathcal{N}_i^{l_2}\}) = \beta_{l_1} \beta_{l_2} \sum_{j \in \mathcal{N}_u^{l_1}} \sum_{v \in \mathcal{N}_i^{l_2}} \alpha_{ju}^{l_1} \alpha_{vi}^{l_2} \mathbf{e}_j^0 \top \mathbf{e}_v^0$ denotes the total strength (i.e.,

¹Detailed derivation is attached in Appendix B.1.

χ) of collaborations (i.e., $C\mathcal{E}$) between nodes in $\mathcal{N}_u^{l_1}$ and nodes in $\mathcal{N}_i^{l_2}$. Therefore, based on Eq. (4), we present the answer to Q_1 as A_1 : *L-layer LightGCN-based message-passing captures and leverages collaborations between nodes $(j, v) \in \bigcup_{l_1=0}^L \mathcal{N}_u^{l_1} \times \bigcup_{l_2=0}^L \mathcal{N}_i^{l_2}$, and the strength of which is determined by 1) $\mathbf{e}_j^0 \mathbf{e}_v^0$: embedding similarity between j and v , 2) $\alpha_{ju}^{l_1} (\alpha_{vi}^{l_2})$: weight of paths from $j(v)$ to $u(i)$, and 3) $\{\beta_l | l \in \{0, 1, 2, \dots, L\}\}$: the weight of each layer.*

Even though users could leverage collaborations from other users/items as demonstrated above, we cannot guarantee all of these collaborations benefit to their rankings. For example in Figure 1(d) where we have a 2-hop subgraph centering around user u and we want to predict the unobserved interaction between u and i in the testing set, after 1-layer message-passing as Figure 1(c) shows, u would leverage collaborations from its three neighbors $\mathcal{N}_u^1 = \{j_1, j_2, j_3\}$ to rank over i . Intuitively, we expect y_{ui} to be higher so that i would be ranked among u 's top- k items. Based on the answer to Q_1 , the strength of each of these three collaborations could be expressed as:

$$\chi(C\mathcal{E}(\{j\}, \bigcup_{l_2=0}^1 \mathcal{N}_i^{l_2})), \forall j \in \mathcal{N}_u^1 = \{j_1, j_2, j_3\} \quad (6)$$

Since j_1 has two common neighbors v_1 and v_2 with item i while j_2 has only one common neighbor v_3 with item i , the embedding similarity between j_1 and any node in $\bigcup_{l_2=0}^1 \mathcal{N}_i^{l_2}$ would be on average higher than the one of j_2 by optimizing Eq. (3) on the observed interactions as demonstrated in Figure 1(b). Therefore, the collaborations from j_1 would contribute more to y_{ui} than the one from j_2 based on Eq. (4). In addition, since j_3 has no common neighbors with i , its embedding similarity to any node in $\bigcup_{l_2=0}^1 \mathcal{N}_i^{l_2}$ would be never optimized to increase² and hence the collaborations from j_3 would not increase y_{ui} . Even worse, incorporating such collaborations could introduce noisy embeddings from unrelated users/items and corrupt u 's embedding, which could further either cause false negative prediction on the link between u and i or introduce some false positive predictions on u 's interested items.

Based on the above analysis, given a center user u , we expect to leverage more collaborations from u 's observed neighboring items that have higher level of interaction (e.g., j_1, j_2 rather than j_3) with u 's interacted but unobserved items in testing set (i.e., i). To mathematically quantify such level of interactions, we propose a graph topological metric, Common Interacted Ratio (CIR), and present its formal definition as follows:

Definition 3.1. Common Interacted Ratio (CIR): For an observed neighboring item $j \in \mathcal{N}_u^1$ of user u , the CIR of j around u , i.e., $\widehat{\phi}_u(j)$, is defined as the averaging interacting ratio over all unobserved neighboring items of u in $\widehat{\mathcal{N}}_u^1$:

$$\widehat{\phi}_u(j) = \mathbb{E}_{i \sim \widehat{\mathcal{N}}_u^1} \frac{|\mathcal{N}_j^1 \cap \mathcal{N}_i^1|}{f(\mathcal{N}_j^1, \mathcal{N}_i^1)}, j \in \mathcal{N}_u^1, u \in \mathcal{U}, \quad (7)$$

where $\mathcal{N}_j^1 \cap \mathcal{N}_i^1$ represents the set of nodes directly co-interacting with j and i based on the observed user-item interactions in training

²Even worse, if j_3 is sampled as a negative pair with any of v_1, v_2, v_3 , its embedding similarity will actually decrease.

Table 1: Average Rank-Biased Overlap of the ranked neighbors between training and testing/full dataset over all nodes.

Metric	Gowalla		Yelp		ML-1M	
	Train-Test	Train-Full	Train-Test	Train-Full	Train-Test	Train-Full
JC	0.604±0.129	0.902±0.084	0.636±0.124	0.897±0.081	0.848±0.092	0.978±0.019
SC	0.611±0.127	0.896±0.084	0.657±0.124	0.900±0.077	0.876±0.077	0.983±0.015
LHN	0.598±0.121	0.974±0.036	0.578±0.100	0.976±0.029	0.845±0.082	0.987±0.009
CN	0.784±0.120	0.979±0.029	0.836±0.100	0.983±0.023	0.957±0.039	0.995±0.006

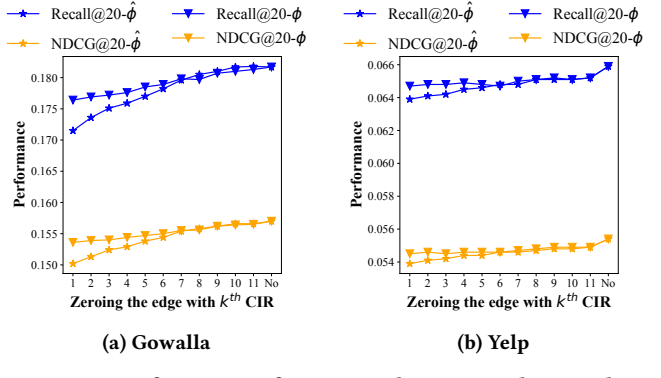


Figure 2: Performance of respectively setting edge weight to be 0 according to the rank of $\widehat{\phi}(\phi)$ where 'no' refers to the original edge weight. Clearly, the higher a neighbor's CIR $\widehat{\phi}(\phi)$, the more beneficial of leveraging its collaboration.

set. To remove the bias that nodes with higher degree typically have a larger number of common interacted items with other nodes, we normalize $|\mathcal{N}_j^1 \cap \mathcal{N}_i^1|$ by $f(\mathcal{N}_j^1, \mathcal{N}_i^1)$, which is a function of j and i 's neighborhood set. Depending on the specific f used here, the CIR could express many existing graph topological metrics for measuring common neighbors, such as Jaccard Similarity (JC) [19], Salton Cosine Similarity (SC) [26], Leicht-Holme-Nerman (LHN) [17] and Common Neighbors (CN) [21]. The detailed computation of these four metrics is attached in the Appendix A.1. Next we empirically verify the importance of passing messages according to $\widehat{\phi}_u(j)$ to the quality of user u 's ranking. We first calculate $\widehat{\phi}_u(j)$ for all edges³ and rank $\{\widehat{\phi}_u(j) | j \in \mathcal{N}_u^1\}, \forall u \in \mathcal{U}$. Then we respectively set the edge weight of the k^{th} neighbor according to $\widehat{\phi}_u(j)$ and re-perform a LightGCN-based ranking with the pretrained user/item embeddings. In Figure 2, we can clearly see that as we void the propagation from neighbors with higher CIR, the whole recommendation performance also decreases, which naturally leads to Q_2 's answer as A_2 : *The benefits to u 's ranking caused by leveraging collaboration from u 's neighboring node j during message-passing increases as CIR $\widehat{\phi}_u(j)$ increases.*

However, leveraging $\widehat{\phi}_u(j)$ to compute edge weights for message-passing is unrealistic since we do not have access to the testing set in advance and hence cannot sample i from $\widehat{\mathcal{N}}_u^1$. Thereby, we propose to approximate $\widehat{\phi}_u(j)$ by sampling k from the observed training set \mathcal{N}_u^1 instead of the unobserved testing set $\widehat{\mathcal{N}}_u^1$ and denote this estimated version as $\phi_u(j)$. Such approximation assumes that for a specific centering node, the neighboring nodes that are more

³Calculating $\widehat{\phi}_u(j)$ for all j centering around corresponding u is equivalent to calculate the weight of all directed edges according to Eq (7).

interacted with other neighboring nodes in the training set would also be more interacted with the neighboring nodes in the testing set. We further empirically justify the correctness of this assumption by comparing the ranking consistence among CIRs calculated by sampling from training neighborhoods (i.e., $\phi_u(j)$), from testing neighborhoods ((i.e., $\phi_u(j)$)) and from full neighborhoods (we replace \hat{N}_u^1 with $N_u^1 \cup \hat{N}_u^1$ in Eq. (7)). Here we respectively use the previous four topological metrics (JS, SC, LHIN, and CN) to define f function and rank the obtained three lists. Then, we measure the similarity of the ranked lists between Train-Test and between Train-Full by Rank-Biased Overlap (RBO) [35]. The averaged RBO values over all nodes $v \in \mathcal{V}$ on three datasets are shown in Table 1. We can clearly see that the RBO values on all these datasets using all topological metrics are beyond 0.5, which verifies our assumption. The RBO value between Train-Full is always higher than the one between Train-Test because most interactions are in training set. Furthermore, in Figure 2, we observe the similar trend of the increasing performance as voiding propagation from neighbors with lower estimated CIR ϕ , which also verifies this approximation.

The answer to Q_2 naturally inspires us to strengthen/weaken the message-passing from neighborhoods with higher/lower CIR. Following this philosophy, we design our Collaboration-Aware Graph Convolution Networks in Section 4. Even though all previous insights are derived upon users, they also apply to items due to the symmetric formulation of LightGCN.

4 COLLABORATION-AWARE GRAPH CONVOLUTIONAL NETWORKS

The former section demonstrates that adjusting the amount of message passed from neighbors based on their CIRs is crucial in improving users' ranking and enhancing the recommendation performance. Driven by these findings, we propose a new graph convolution operation, Collaboration-Aware Graph Convolution(CAGC), which selectively passes node messages based on the benefits of their corresponding collaborations. Furthermore, we wrap the proposed CAGC within the existing framework of LightGCN and develop the class of Collaboration-Aware Graph Convolutional Networks.

The core idea of CAGC is to strengthen/weaken the messages passed from neighbors with higher/lower CIR to center nodes. To achieve this, we compute the edge weight for message-passing as:

$$\Phi_{ij} = \begin{cases} \phi_i(j), & \text{if } A_{ij} > 0 \\ 0, & \text{if } A_{ij} = 0 \end{cases}, \forall i, j \in \mathcal{V} \quad (8)$$

where $\phi_i(j)$ is the CIR of neighboring node j centering around i . Note that unlike the graph convolution $D^{-0.5}AD^{-0.5}$ used in LightGCN which is symmetric, here Φ is unsymmetrical. This is rather interpretable: the interacting level of node j with neighborhood of node i is likely to be different from the interacting level of node i with neighborhood of node j . Similar to calculating edge attention [29], we normalize Φ by the total message weights collected at i and propagating node embeddings as:

$$\mathbf{e}_i^{l+1} = \sum_{j \in \mathcal{N}_i^1} \gamma_i \frac{\Phi_{ij}}{\sum_{k \in \mathcal{N}_i^1} \Phi_{ik}} \mathbf{e}_j^l, \forall i \in \mathcal{V} \quad (9)$$

where α_i is a coefficient that allows us to flexibly vary the total amount of message flowing to each node and further control the

embedding magnitude of that node. As demonstrated in [22], the embedding magnitude is crucial to the performance of recommendation. However, aggregating messages according to edge weights computed by Eq. (9) without γ_i would significantly change the magnitude of embedding. Therefore, to guarantee that the total amount of message collected at each node after incorporating CIR equals to the one in LightGCN, we set $\gamma_i = \sum_{k \in \mathcal{N}_i^1} d_i^{-0.5} d_k^{-0.5}$.

Furthermore, we borrow the idea of and multi-view learning [42] to augment the current CAGC. Specifically, we treat the message-passing following edge weights calculated according to the original LightGCN and the proposed CAGC as two separate views that capture different types of collaborations, and then fuse them together to form our final Augmented Collaboration Aware Graph Convolution (CAGC*):

$$\mathbf{e}_i^{l+1} = \sum_{j \in \mathcal{N}_i^1} g(\gamma_i \frac{\Phi_{ij}}{\sum_{k \in \mathcal{N}_i^1} \Phi_{ik}}, d_i^{-0.5} d_j^{-0.5}) \mathbf{e}_j^l, \forall i \in \mathcal{V} \quad (10)$$

where g is a function combining the edge weights for propagating embeddings according to CAGC and LightGCN. We could either learn g by parametrization (e.g., concatenating these two types of propagated embeddings and applying MLP to guarantee the universal approximation of g [36, 39]) or set g based on prior knowledge (e.g., weighted sum these two propagated embeddings). Specifics of g for the experiments in this work are discussed in Section 5.1.4.

To further enhance the intuition of CAGC*, we theoretically prove that GNNs whose aggregation scheme is CAGC* can be more expressive than 1-WL. First, we demonstrate the equivalence between the subtree-isomorphism and the subgraph-isomorphism in bipartite graphs⁴:

THEOREM 4.1. *In bipartite graphs, two subgraphs that are subtree-isomorphic if and only if they are subgraph-isomorphic.*

Given the fact that 1-WL test can distinguish subtree-isomorphic graphs [36], the equivalence between these two isomorphisms disclosed by Theorem 4.1 indicates that in bipartite graphs, both of the subtree-isomorphic graphs and subgraph-isomorphic graphs can be distinguished by 1-WL test. Therefore, to go beyond 1-WL in bipartite graphs, we propose a novel bipartite-subgraph-isomorphism in Definition 4.1, which is even harder to be distinguished than the subgraph-isomorphism by 1-WL test. Intuitively, two subgraphs that are isomorphic in a bipartite graph would need to share similar 2nd-hop topological pattern:

Definition 4.1. Bipartite-subgraph-isomorphism: S_u and S_i are bipartite-subgraph-isomorphic, denoted as $S_u \cong_{bi-subgraph} S_i$, if there exists a bijective mapping $h : \tilde{N}_u^1 \cup N_u^2 \rightarrow \tilde{N}_i^1 \cup N_i^2$ such that $h(u) = i$ and $\forall v, v' \in \tilde{N}_u^1 \cup N_u^2, e_{vv'} \in \mathcal{E} \iff e_{h(v)h(v')} \in \mathcal{E}$ and $\mathbf{e}_v^l = \mathbf{e}_{h(v)}^l, \mathbf{e}_{v'}^l = \mathbf{e}_{h(v')}^l$.

With these two definitions, we formally propose Theorem 4.2 to prove that GNNs whose aggregation scheme is CAGC* can be more expressive than 1-WL in distinguishing subtree (subgraph)-isomorphic yet non-bipartite-subgraph-isomorphic graphs, i.e., CAGC* can distinguish non-bipartite-subgraph-isomorphic graphs that are indistinguishable by 1-WL.

⁴The definition of subtree-isomorphism/subgraph-isomorphism and the proof of their equivalence in bipartite graphs are included in Appendix A.2 and B.2.

THEOREM 4.2. Let M be a GNN whose aggregation scheme is CAGC* defined by Eq. (10). M is strictly more expressive than 1-WL in distinguishing subtree-isomorphic yet non-bipartite-subgraph-isomorphic graphs if M has a sufficient number of layers and also satisfies the following two conditions:

- (1) M can distinguish at least two neighborhood subgraphs S_u and S_i with $S_u \cong_{\text{subtree}} S_i$, $S_u \not\cong_{\text{bi-subgraph}} S_i$ and $\{\Phi_{uv} | v \in N_u, u \in \mathcal{U}\} \neq \{\Phi_{ij} | j \in N_i, i \in \mathcal{I}\}$.
- (2) $g(\{(y_i \tilde{\Phi}_{ij}, e_j^l) | j \in N_i^1\}, \{(d_i^{-0.5} d_j^{-0.5}, e_j^l) | j \in N_i^1\})$ is injective.

The detailed proof of Theorem 4.2 is attached in Appendix B.3. The 1st-condition is satisfied by the example shown in Figure 7 and the 2nd-condition is satisfied by Lemma 1 in assuming node embeddings share the same discretization precision [36, 39]. Theorem 4.2 indicates that if we pass messages according to CAGC*, the representations of two nodes that are originally indistinguishable due to the same structure of their neighborhood subgraphs would become distinguishable by capturing CIRs of neighborhoods. Note that it is crucial to add the LightGCN-based message-passing to guarantee the injectivity of the embedding function h . *To the best of our knowledge, this is the first work proposing the concept of bipartite-subgraph-isomorphism and designing a graph convolution CAGC* that can go beyond 1-WL in differentiating such type of isomorphism in bipartite graphs.*

Following the principle of LightGCN that the designed graph convolution should be light and easy to train, all other components of our architecture except the message-passing is exactly the same as LightGCN, which have already been covered in Section 2 and hence we omit the description for brevity and refer readers to Appendix C for more details. We visualize our CAGC* in Figure 3. Clearly, our model shares the same time/space complexity with LightGCN in all components except the graph convolution operation. However, we can pre-calculate Φ before the whole training process starts, and the extra time complexity of this pre-calculation would be minor compared with the whole training process. Furthermore, by Eq. (8), Φ shares the same sparsity as $D^{-0.5}AD^{-0.5}$, and then the space to save the extra Φ would also be asymptotically same as the space for saving $D^{-0.5}AD^{-0.5}$. Even better, since CAGC* could capture more beneficial collaborations as justified by the answer to Q_2 and is more expressive than the 1-WL test in differentiating bipartite-subgraph-isomorphism as justified by Theorem 4.2, our proposed CAGC* would achieve higher performance with significantly less time and fewer training epochs. These benefits drastically impulse the practical usage of CAGC* in industry-level applications. We will empirically demonstrate all of these advantages in Section 5.

5 EXPERIMENTS

In this section, we conduct extensive experiments to evaluate the effectiveness of our proposed CAGC(*) variants.

5.1 Experimental Settings

5.1.1 Datasets. Following [11, 30], we validate the proposed approach on four widely used benchmark datasets in recommender systems, including **Gowalla**, **Yelp**, **Amazon**, and **MI-1M**, the details of which are provided in [11, 30]. Moreover, we collect two extra datasets to further demonstrate the superiority of our proposed model in even broader user-item interaction domains:

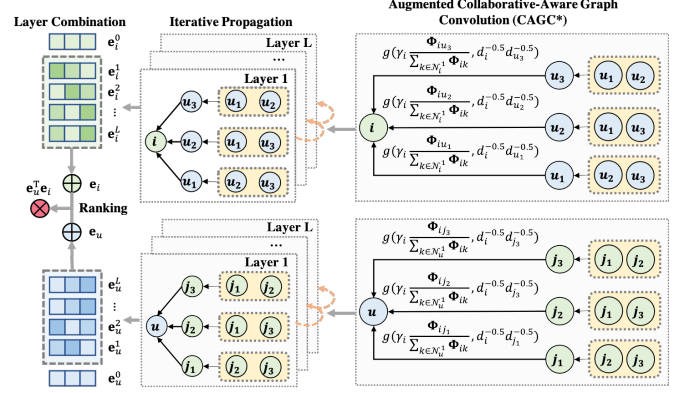


Figure 3: The architecture of the proposed Augmented Collaboration-Aware Graph Convolution Network.

Table 2: Basic dataset statistics.

Dataset	# Users	# Items	# Interactions	Density
Gowalla	29,858	40,981	1,027,370	0.084%
Yelp	31,668	38,048	1,561,406	0.130%
Amazon	52,643	91,599	2,984,108	0.062%
MI-1M	6,022	3,043	895,699	4.888%
Loseit	5,334	54,595	230,866	0.08%
News	29,785	21,549	766,874	0.119%

*Yelp: Yelp2018; *Amazon: Amazon-Books; *MI-1M: MovieLens-1M.

(1) Loseit: This dataset is collected from subreddit *loseit - Lose the Fat*⁵ from March 2020 to March 2022 where users discuss healthy and sustainable methods of losing weight via posts. To ensure the quality of this dataset, we use the 10-core setting [10], i.e., retaining users and posts with at least ten interactions. **(2) News:** This dataset includes the interactions from subreddit *World News*⁶ where users share major news around the world via posts. Similarly, we use the 10-core setting to ensure the quality of this dataset. We summarize the statistics of all six datasets in Table 2.

5.1.2 Baselines. We compare our proposed CAGC(*) with the following baselines:

- **MF** [24]: This is the most classic collaborative filtering method equipped with the BPR loss [24], which preserves users' ranking over interacted items with respect to uninteracted items.
- **NGCF** [30]: This was the very first GNN-based collaborative filtering model to incorporate high-order connectivity of user-item interactions for recommendation.
- **LightGCN** [11]: This is the most popular collaborative filtering model based on GNNs, which extends NGCF by removing feature transformation and nonlinear activation, and achieves better trade-off between the performance and efficiency.
- **UltraGCN** [20]: This model simplifies GCNs for collaborative filtering by omitting infinite layers of message passing for efficient recommendation, and it constructs the user-user graphs to leverage higher-order relationships. Thus, it achieves both better performance and shorter running time than LightGCN.
- **GTN** [6]: This model leverages a robust and adaptive propagation based on the trend of the aggregated messages to avoid the unreliable user-item interactions.

⁵<https://www.reddit.com/r/loseit/>

⁶<https://www.reddit.com/r/worldnews/>

Table 3: Performance comparison of CAGCN(*) with baselines. The best and runner-up results are colored in red and blue.

Model	Metric	MF	NGCF	LightGCN	UltraGCN	CAGCN			CAGCN*		
		-jc	-sc	-cn	-lhn	-jc	-sc	-lhn	-jc	-sc	-lhn
Gowalla	Recall@20	0.1554	0.1563	0.1817	0.1867	0.1825	0.1826	0.1632	0.1821	0.1878	0.1878
	NDCG@20	0.1301	0.1300	0.1570	0.1580	0.1575	0.1577	0.1381	0.1577	0.1591	0.1588
Yelp2018	Recall@20	0.0539	0.0596	0.0659	0.0675	0.0674	0.0671	0.0661	0.0661	0.0708	0.0711
	NDCG@20	0.0460	0.0489	0.0554	0.0553	0.0564	0.0560	0.0546	0.0555	0.0586	0.0590
Amazon	Recall@20	0.0337	0.0336	0.0420	0.0682	0.0435	0.0435	0.0403	0.0422	0.0510	0.0506
	NDCG@20	0.0265	0.0262	0.0331	0.0553	0.0343	0.0342	0.0321	0.0333	0.0403	0.0400
ML-1M	Recall@20	0.2604	0.2619	0.2752	0.2783	0.2780	0.2786	0.2730	0.2760	0.2822	0.2827
	NDCG@20	0.2697	0.2729	0.2820	0.2638	0.2871	0.2881	0.2818	0.2871	0.2775	0.2776
Loseit	Recall@20	0.0539	0.0574	0.0588	0.0621	0.0622	0.0625	0.0502	0.0592	0.0654	0.0658
	NDCG@20	0.0420	0.0442	0.0465	0.0446	0.0474	0.0470	0.0379	0.0461	0.0486	0.0484
News	Recall@20	0.1942	0.1994	0.2035	0.2034	0.2135	0.2132	0.1726	0.2084	0.2182	0.2172
	NDCG@20	0.1235	0.1291	0.1311	0.1301	0.1385	0.1384	0.1064	0.1327	0.1405	0.1414
Avg. Rank	Recall@20	9.83	9.17	7.33	4.17	4.67	4.33	8.83	6.17	1.67	1.50
	NDCG@20	9.50	9.17	5.83	6.00	3.67	4.00	8.33	5.00	2.50	2.50

Note that here we only compare the proposed CAGCN(*) with the baselines that focus on the operation of graph convolution (besides the classic MF) including the state-of-the-art GNN-based recommendation models (i.e., UltraGCN and GTN). There are some other developing methodology directions (e.g., [1–3, 7]) that can obtain comparable results to the aforementioned baselines on some of the benchmark datasets. However, these methods are either not GNN-based [7] or incorporates some other general machine learning techniques rather than focus on graph convolution, e.g., SGNCNs [1] leverages the stochastic binary masks to remove noisy edges, and GOTNet [2] performs k-Means clustering on nodes’ embeddings to capture long-range dependencies. Given our main focus is on advancing the frontier of graph-convolution in recommendation systems, we omit these other comparable baselines. Note that our work could be further enhanced if incorporating these general machine learning techniques but we leave this as one future direction.

5.1.3 Evaluation Metrics. Two popular metrics: Recall@K and Normalized Discounted Cumulative Gain (NDCG@K) [30] are adopted to evaluate all models. We set the default value of K as 20 and report the average of Recall@20 and NDCG@20 over all users in the test set. In the inference phase, we treat items that the user has never interacted with in training set as candidate items. All recommendation models predict the user’s preference scores over these candidate items and rank them based on the computed scores to further calculate Recall@20 and NDCG@20.

5.1.4 Hyperparameter Settings. We strictly follow the experimental setting used in LightGCN [11] to ensure the fair comparison. For all other models, we adopt exactly the same hyper-parameters as suggested by the corresponding papers for all baselines to avoid any biased comparison: the embedding size $d^0 = 64$, learning rate $lr = 0.001$, the number of propagating layers $L = 3$, training batch size 2048. The coefficient of l2-regularization is searched in $\{1e^{-4}, 1e^{-3}\}$. As the user/item embedding is the main network parameter, it is crucial to ensure the same embedding size for fair comparison between different models. Therefore, when comparing with GTN [6], we set the embedding size to be 256 to align with [6].

For CAGCN, we set γ_i as $\sum_{j \in \mathcal{N}_i^1} d_i^{-0.5} d_j^{-0.5}$ to ensure the same embedding magnitude as LightGCN. For CAGCN*, we set g as the weighted sum in Eq. (10) for efficiency/less computation. Although using the weighted sum cannot guarantee the universal approximation of g as MLP [39], we empirically find it still achieves superior performance over existing work. Furthermore, we set $\gamma_i = \gamma$ as a constant controlling the contributions of capturing different collaborations. Note that we search the optimal γ within $\{1, 1.2, 1.5, 1.7, 2.0\}$. In addition, we term the model variant as CAGCN(*)-jc if we use JC to compute ϕ . The same rule applies to other topological metrics. Our code is available at <https://github.com/YuWVandy/CAGCN>.

5.2 Performance Comparison

We first compare our proposed CAGCN-variants with LightGCN to demonstrate its advantages in capturing beneficial collaboration. Clearly from Table 3, CAGCN-jc/sc/lhn achieves higher performance than LightGCN. This is because we selectively propagate node embeddings by the proposed CIR metrics (JS, SC, LHN). Then the corresponding CAGC convolution would be aware of capturing collaborations of which neighbors would be most beneficial, i.e., would increase users’ ranking over user-interested items the most. However, CAGCN-cn mostly performs worse than LightGCN because nodes having more common neighbors with other nodes are more likely to have higher degrees and hence connect with more unrelated nodes. If we blindly propagate more messages from these higher degree nodes according to CN without removing this degree-related bias, the corresponding CAGC convolution would capture uninformative or even harmful collaborative signals, which corrupts user/item embeddings and cause false-positive link predictions. Moreover, CAGCN-js and CAGCN-sc are mostly better than CAGCN-lhn. This is because LHN is more sensitive to node degree than JS and SC as justified in Appendix A.1, and hence the amount of messages passed according to LHN would be weakly determined by the number of common neighbors while strongly determined by the node degree. Therefore, CAGCN-lhn fails to selectively pass messages based on the benefits of captured collaborations. Comparing LHN with CN, the former emphasizes more on node degrees while the latter emphasizes more on absolute number of common

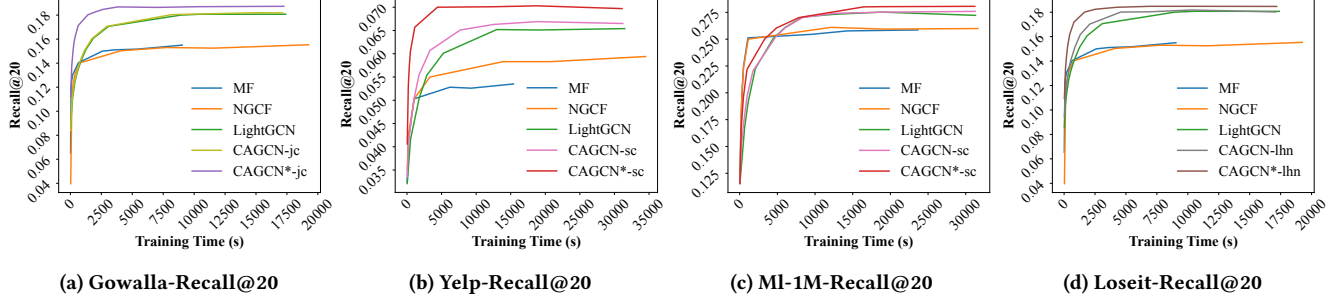


Figure 4: Comparing the training time of CAGCN(*) with other baselines on four datasets. For clear visualization, we only report the efficiency of the best CAGCN(*) variant based on Table 3 for each dataset. CAGCN* almost always achieves extremely higher Recall@20 with significant less time. Note that we observe a similar trend across the datasets for NDCG@20 and report the results in Figure 8 in Appendix E.1.

Table 4: Performance comparison of CAGCN* with GTN.

Model	Metric	GTN	CAGCN*		
			-jc	-sc	-lnh
Gowalla	Recall@20	0.1870	0.1901	0.1899	0.1885
	NDCG@20	0.1588	0.1604	0.1603	0.1576
Yelp2018	Recall@20	0.0679	0.0731	0.0729	0.0689
	NDCG@20	0.0554	0.0605	0.0601	0.0565
Amazon	Recall@20	0.0450	0.0573	0.0575	0.0520
	NDCG@20	0.0346	0.0456	0.0458	0.0409

neighbors, both of which are inferior in capturing beneficial collaborations to JS and SC. Since different datasets exhibit different patterns of 2nd-order connectivity, i.e., how items are connected with other items through interacting with intermediate users, there is no fixed topological metric that performs the best among all datasets. For example, CAGCN-jc performs better than CAGCN-sc on Yelp and News, while worse on Gowalla, MI-1M and Loseit. Then, we compare CAGCN(*)-variants with other competing baselines. We omit CAGCN*-cn here due to the worse performance of CAGCN-cn than LightGCN. We can see that CAGCN*-jc/sc almost consistently achieves higher performance than other baselines except UltraGCN on Amazon. This is because UltraGCN allows multiple negative samples for each positive interaction, e.g., 500 negative samples here on Amazon⁷, which lowers the efficiency as we need to spend more time preparing such large number of negative samples per epoch. Among the baselines, UltraGCN exhibits the strongest performance because it approximates the infinite layers of message passing and constructs the user-user graphs to leverage higher-order relationships. LightGCN and NGCF generally perform better than MF-BPR since they inject the collaborative effect directly through message-passing. Furthermore, we increase the embedding size d^0 to 256 following [6]⁸ and observe the consistent superiority of our model over GTN in Table 4. This is because in GTN [6], the edge weights for message-passing are still computed based on node embeddings that implicitly encode noisy collaborative signals from unreliable interactions. Conversely, our CAGCN* directly alleviates the propagation on unreliable interactions based on its CIR value, which removes noisy interactions from the source.

⁷UltraGCN uses 1500/800/500 negative samples for Gowalla/Yelp2018/Amazon datasets

⁸As the user/item embedding is the main network parameters, it is crucial to ensure the same embedding size when comparing different models and hence we use the exactly the same embedding size as GTN.

Table 5: Efficiency comparison of CAGCN* with LightGCN.

Model	Stage	Gowalla	Yelp	Amazon*	MI-1M	Loseit	News
LightGCN	Training	16432.0	28788.0	81976.5	18872.3	39031.0	13860.8
	Preprocess	167.4	281.6	1035.8	33.8	31.4	169.0
	Total	2963.2	1904.4	1983.9	11304.7	10417.7	1088.4
CAGCN*	Training	3130.6	2186.0	3019.7	11338.5	10449.1	1157.4
	Total	82.0%	93.4%	97.6%	40.1%	73.3%	92.1%
Improve	Training	80.9%	92.4%	96.3%	39.9%	73.2%	91.6%
	Total						

* Unlike other datasets where we have enough RAM and hence can parallelly pre-compute CIR in the matrix form, our RAM is not enough for Amazon and hence we compute CIR sequentially for each node. Therefore, the preprocessing time for Amazon is longer than other datasets, which even so is still significantly less than the training time of LightGCN.

5.3 Efficiency Comparison

As recommendation models will be eventually deployed in user-item data of real-world scale, it is crucial to compare the efficiency of the proposed CAGCN(*) with other baselines. For fair comparison, we use a uniform code framework implemented ourselves for all models and run them on the same machine with Ubuntu 20.04 system, AMD Ryzen 9 5900 12-Core Processor, 128 GB RAM and GPU NVIDIA GeForce RTX 3090. For clear visualization, we only report the Recall@20 of the best CAGCN(*) variant based on Table 3 and the corresponding NDCG@20 is included in Appendix E.1. Clearly in Figure 4, CAGCN(*) achieves extremely higher performance in significant less time. This is because the designed graph convolution could recognize neighbors whose collaborations are most beneficial to users' ranking and by passing more messages from these neighbors, our model can achieve higher performance with less training time. An interesting observation is that unlike other three datasets, Recall@20 of LightGCN and CAGCN(*) on MI-1M increases slower than other models in the first 3000s. We hypothesize that at the initial training stage, the higher density of MI-1M as in Table 2 leads to aggregating so many noisy neighboring nodes' information together and causes false positive prediction. However, later when keeping optimizing based on newly-sampled negative pairs, LightGCN and CAGCN(*) can maintain the separability of embeddings between users and their uninterested items.

Furthermore, we report the first time that our best CAGCN* variant achieving the best performance of LightGCN on each dataset in Table 5. To ensure the fair comparison, we also include the time for precomputing CIR matrix as the preprocess time for our CAGCN*. We could see CAGCN* spends significant less time to achieve the same best performance as LightGCN, which highlights the broad prospects to deploy CAGCN* in real-world recommendations.

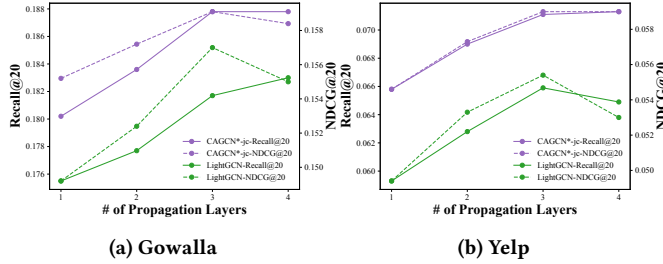


Figure 5: Results of different propagation layers.

5.4 Further Probe

5.4.1 *What are the impacts of changing propagation layers?* We increase the propagation layer of CAGCN* and LightGCN from 1 to 4 and visualize their corresponding performance in Figure 5. Clearly, the performance first increases as layer increases from 1 to 3 and then decreases on both Gowalla and Yelp2018, which is consistent with [11]’s finding. More importantly, our CAGCN* is always better than LightGCN at all propagation layers.

5.4.2 *Interpretation on the advantages of CAGCN(*)*. Here we visualize the performance of all models for nodes in different degree groups. Comparing non-graph-based methods (e.g., MF), graph-based methods (e.g., LightGCN, CAGCN(*)) achieve higher performance for lower degree nodes [0, 300) while lower performance for higher degree nodes [300, Inf). Because the node degrees follow the power-law distribution [27], the average performance of graph-based methods would still be higher. To the best of our knowledge, this is the first work discovering such performance imbalance/unfairness issue w.r.t. node degree in graph-based recommendation models. On one hand, graph-based models could leverage neighborhood information to augment the weak supervision for low-degree (cold-start) nodes. On the other hand, it would introduce many noisy/unreliable interactions for higher-degree nodes. It is crucial to design an unbiased graph-based recommendation model that can achieve higher performance on both low and high degree nodes. In addition, the opposite performance trends between NDCG and Recall indicates that different evaluation metrics have different levels of sensitivity to node degrees.

6 RELATED WORK

6.1 Collaborative Filtering (CF)

As an effective tool for personalized recommendation, CF assumes that people sharing similar interest on one thing tend to have the same preference on another thing, and it predicts the interest of a user (filtering) by utilizing the preference from other users who have similar interests (collaborative) [8]. Early CF methods used MF techniques [23], which generally map the IDs of users and items to a joint latent factor space and take the inner product of the embeddings to estimate the user-item interactions [16, 24]. Despite the initial success, these methods failed to capture the nonlinear user-item relationships due to their intrinsic linearity. To address this issue, deep learning was used to capture the non-linearity (e.g. by replacing the linear inner product operation with the nonlinear neural networks) [28, 30]. All above methods capture CF effect by optimizing embedding similarity based on observed user-item

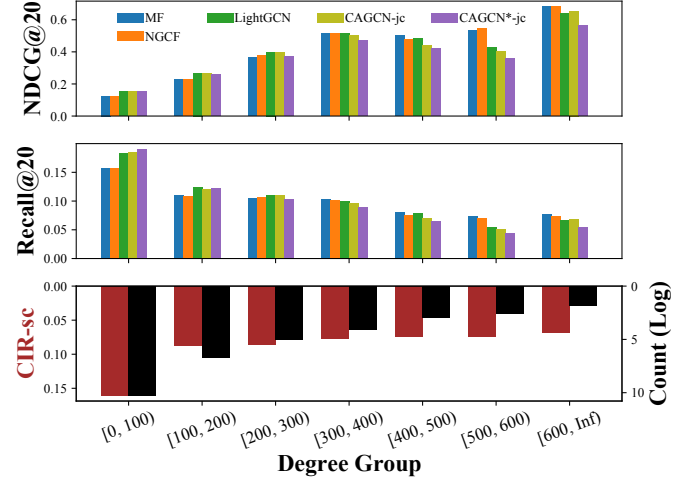


Figure 6: The performance of each model w.r.t. node degree on Gowalla. Note that we observe the similar trend on Yelp in Figure 9 in Appendix E.2.

interactions. Stepping further, graph-based methods are proposed to leverage message-passing to directly inject the CF effect into the user/item embeddings [11, 30].

6.2 Graph-based Methods for Recommendation

Since user-item interaction can be naturally modeled as a bipartite graph, another line of research [9, 11, 12, 30] infers users’ preferences by exploring the topological patterns of user-item bipartite graphs. Two pioneering work, ItemRank [9] and BiRank [12], define users’ preferences based on their observed interacted items and perform label propagation to capture the CF effect. Although users’ ranking scores are computed based on structural proximity between the observed items and the target item, the non-trainable user preferences and the lack of recommendation-based objectives in these methods lead to inferior performance to embedding-based methods such as MF-BPR [24]. Furthermore, HOP-Rec [40] combines the graph-based methods, which better capture the collaboration among nodes, and embedding-based methods, which better optimize the recommendation objective function. Yet, interactions captured by random walks do not fully explore the high-layer neighbors and multi-hop dependencies [33]. By contrast, GNN-based recommendation methods are superior at encoding structural proximity (especially higher-order connection) in user/item embeddings, which is crucial in capturing the CF effect [6, 11, 30]. For example, SGL [38] further leverages contrastive learning [34] with graph augmentation to enhance model robustness against noisy interactions, but it still follows the existing message-passing mechanism of GNNs without any justification. In fact, all of these GNN-based models directly borrow the traditional graph convolution operation from node/graph classification and blindly propagate neighboring users/items embeddings without any recommendation-tailored modification. Actually, our work has demonstrated that the collaboration captured by message-passing may not always improve users’ ranking over items, which inspires us to design a new generation of graph convolutions that adaptively pass messages based on the benefits provided by the captured collaborations.

7 CONCLUSION

In this paper, we find that the message-passing captures collaborative effect by leveraging interactions between neighborhoods. The strength of the captured collaborative effect depends the embedding similarity, the weight of paths and the contribution of each propagation layer. Then, to determine whether the captured collaborative effect would benefit the prediction of user preferences, we further propose the Common Interacted Ratio (CIR) and empirically verify that leveraging collaborations from neighbors with higher CIR would contribute more to users' ranking. Inspired by our empirical and theoretical observation, we propose CAGCN(*) to selectively aggregate neighboring nodes' information based on their CIRs. We further define a new type of isomorphism, bipartite-subgraph-isomorphism, and prove that our CAGCN* can be more expressive than 1-WL in distinguishing subtree(subgraph)-isomorphic yet non-bipartite-subgraph-isomorphic graphs. Experimental results demonstrate the advantages of the proposed CAGCN(*) over other baselines. Specifically, CAGCN* outperforms the most representative graph-based recommendation model, LightGCN [11], by 9% in Recall@20 but also achieves more than 79% speedup. In the future, we plan to explore the imbalanced performance improvement among nodes in different degree groups as observed in Figure 6 especially from a GNN fairness perspective [32].

REFERENCES

- [1] Huiyuan Chen, Lan Wang, Yusan Lin, Chin-Chia Michael Yeh, Fei Wang, and Hao Yang. 2021. Structured graph convolutional networks with stochastic masks for recommender systems. In *Proceedings of the 44th International ACM SIGIR Conference on Research and Development in Information Retrieval*. 614–623.
- [2] Huiyuan Chen, Chin-Chia Michael Yeh, Fei Wang, and Hao Yang. 2022. Graph Neural Transport Networks with Non-local Attentions for Recommender Systems. In *Proceedings of the ACM Web Conference 2022*. 1955–1964.
- [3] Huiyuan Chen, Kaixiong Zhou, Kwei-Herng Lai, Xia Hu, Fei Wang, and Hao Yang. 2022. Adversarial Graph Perturbations for Recommendations at Scale. (2022).
- [4] Paul Covington, Jay Adams, and Emre Sargin. 2016. Deep neural networks for youtube recommendations. In *Proceedings of the 10th ACM conference on recommender systems*. 191–198.
- [5] Travis Ebessu, Bin Shen, and Yi Fang. 2018. Collaborative memory network for recommendation systems. In *The 41st international ACM SIGIR conference on research & development in information retrieval*. 515–524.
- [6] Wenqi Fan, Xiaorui Liu, Wei Jin, Xiangyu Zhao, Jiliang Tang, and Qing Li. 2021. Graph Trend Networks for Recommendations. *arXiv preprint arXiv:2108.05552* (2021).
- [7] Hao-Ming Fu, Patrick Poirson, Kwot Sin Lee, and Chen Wang. 2022. Revisiting Neighborhood-based Link Prediction for Collaborative Filtering. *arXiv preprint arXiv:2203.15789* (2022).
- [8] David Goldberg, David Nichols, Brian M Oki, and Douglas Terry. 1992. Using collaborative filtering to weave an information tapestry. *Commun. ACM* 35, 12 (1992), 61–70.
- [9] Marco Gori, Augusto Pucci, V Roma, and I Siena. 2007. Itemrank: A random-walk based scoring algorithm for recommender engines.. In *IJCAI*, Vol. 7. 2766–2771.
- [10] Ruining He and Julian McAuley. 2016. VBPR: visual bayesian personalized ranking from implicit feedback. In *Proceedings of the AAAI Conference on Artificial Intelligence*, Vol. 30.
- [11] Xiangnan He, Kuan Deng, Xiang Wang, Yan Li, Yongdong Zhang, and Meng Wang. 2020. Lightgc: Simplifying and powering graph convolution network for recommendation. In *Proceedings of the 43rd International ACM SIGIR conference on research and development in Information Retrieval*. 639–648.
- [12] Xiangnan He, Ming Gao, Min-Yen Kan, and Dingxian Wang. 2016. Birank: Towards ranking on bipartite graphs. *IEEE Transactions on Knowledge and Data Engineering* 29, 1 (2016), 57–71.
- [13] Xiangnan He, Lizi Liao, Hanwang Zhang, Liqiang Nie, Xia Hu, and Tat-Seng Chua. 2017. Neural collaborative filtering. In *Proceedings of the 26th international conference on world wide web*. 173–182.
- [14] Thomas N. Kipf and Max Welling. 2017. Semi-Supervised Classification with Graph Convolutional Networks. In *ICLR*.
- [15] Johannes Klicpera, Aleksandar Bojchevski, and Stephan Günnemann. 2019. Predict then Propagate: Graph Neural Networks meet Personalized PageRank. In *7th International Conference on Learning Representations, ICLR*.
- [16] Yehuda Koren, Robert Bell, and Chris Volinsky. 2009. Matrix factorization techniques for recommender systems. *Computer* 42, 8 (2009), 30–37.
- [17] Elizabeth A Leicht, Petter Holme, and Mark EJ Newman. 2006. Vertex similarity in networks. *Physical Review E* 73, 2 (2006), 026120.
- [18] Xin Li and Hsinchun Chen. 2013. Recommendation as link prediction in bipartite graphs: A graph kernel-based machine learning approach. *Decision Support Systems* 54, 2 (2013), 880–890.
- [19] David Liben-Nowell and Jon Kleinberg. 2007. The link-prediction problem for social networks. *Journal of the American society for information science and technology* 58, 7 (2007), 1019–1031.
- [20] Kelong Mao, Jieming Zhu, Xi Xiao, Biao Lu, Zhaowei Wang, and Xiuqiang He. 2021. UltraGCN: Ultra Simplification of Graph Convolutional Networks for Recommendation. In *Proceedings of the 30th ACM International Conference on Information & Knowledge Management*. 1253–1262.
- [21] Mark EJ Newman. 2001. Clustering and preferential attachment in growing networks. *Physical review E* 64, 2 (2001), 025102.
- [22] Dongmin Park, Hwanjun Song, Minseok Kim, and Jae-Gil Lee. 2020. TRAP: Two-level regularized autoencoder-based embedding for power-law distributed data. In *Proceedings of The Web Conference 2020*. 1615–1624.
- [23] Steffen Rendle, Christoph Freudenthaler, Zeno Gantner, and Lars Schmidt-Thieme. 2009. BPR: Bayesian personalized ranking from implicit feedback. In *Proceedings of the Twenty-Fifth Conference on Uncertainty in Artificial Intelligence*. 452–461.
- [24] Steffen Rendle, Christoph Freudenthaler, Zeno Gantner, and Lars Schmidt-Thieme. 2012. BPR: Bayesian personalized ranking from implicit feedback. *arXiv preprint arXiv:1205.2618* (2012).
- [25] Francesco Ricci, Lior Rokach, and Bracha Shapira. 2011. Introduction to recommender systems handbook. In *Recommender systems handbook*. Springer.
- [26] Gerard Salton. 1989. Automatic text processing: The transformation, analysis, and retrieval of. *Reading: Addison-Wesley* 169 (1989).
- [27] Andrew T Stephen and Olivier Toubia. 2009. Explaining the power-law degree distribution in a social commerce network. *Social Networks* 31, 4 (2009), 262–270.
- [28] Yi Tay, Luu Anh Tuan, and Siu Cheung Hui. 2018. Latent relational metric learning via memory-based attention for collaborative ranking. In *WWW*. 729–739.
- [29] Petar Veličković, Guillem Cucurull, Arantxa Casanova, Adriana Romero, Pietro Lio, and Yoshua Bengio. 2017. Graph attention networks. *arXiv preprint arXiv:1710.10903* (2017).
- [30] Xiang Wang, Xiangnan He, Meng Wang, Fuli Feng, and Tat-Seng Chua. 2019. Neural graph collaborative filtering. In *Proceedings of the 42nd international ACM SIGIR conference on Research and development in Information Retrieval*. 165–174.
- [31] Xiang Wang, Hongye Jin, An Zhang, Xiangnan He, Tong Xu, and Tat-Seng Chua. 2020. Disentangled graph collaborative filtering. In *Proceedings of the 43rd international ACM SIGIR conference on research and development in information retrieval*. 1001–1010.
- [32] Yu Wang. 2022. Fair Graph Representation Learning with Imbalanced and Biased Data. In *Proceedings of the Fifteenth ACM International Conference on Web Search and Data Mining*.
- [33] Yu Wang and Tyler Derr. 2021. Tree decomposed graph neural network. In *Proceedings of the 30th ACM International Conference on Information & Knowledge Management*. 2040–2049.
- [34] Yu Wang, Wei Jin, and Tyler Derr. 2022. Graph neural networks: Self-supervised learning. In *Graph Neural Networks: Foundations, Frontiers, and Applications*. Springer, 391–420.
- [35] William Webber, Alistair Moffat, and Justin Zobel. 2010. A similarity measure for indefinite rankings. *ACM Transactions on Information Systems (TOIS)* 28, 4 (2010), 1–38.
- [36] Asiri Wijesinghe and Qing Wang. 2021. A New Perspective on " How Graph Neural Networks Go Beyond Weisfeiler-Lehman? ". In *ICLR*.
- [37] Jiancan Wu, Xiang Wang, Fuli Feng, Xiangnan He, Liang Chen, Jianxun Lian, and Xing Xie. 2021. Self-supervised graph learning for recommendation. In *Proceedings of the 44th International ACM SIGIR Conference on Research and Development in Information Retrieval*. 726–735.
- [38] Jiancan Wu, Xiang Wang, Fuli Feng, Xiangnan He, Liang Chen, Jianxun Lian, and Xing Xie. 2021. Self-supervised graph learning for recommendation. In *Proceedings of the 44th International ACM SIGIR Conference on Research and Development in Information Retrieval*. 726–735.
- [39] Keyulu Xu, Weihua Hu, Jure Leskovec, and Stefanie Jegelka. 2018. How powerful are graph neural networks? *arXiv preprint arXiv:1810.00826* (2018).
- [40] Jheng-Hong Yang, Chih-Ming Chen, Chuan-Ju Wang, and Ming-Feng Tsai. 2018. HOP-rec: high-order proximity for implicit recommendation. In *Proceedings of the 12th ACM Conference on Recommender Systems*. 140–144.
- [41] Rex Ying, Ruining He, Kaifeng Chen, Pong Eksombatchai, William L Hamilton, and Jure Leskovec. 2018. Graph convolutional neural networks for web-scale recommender systems. In *Proceedings of the 24th ACM SIGKDD*. 974–983.
- [42] Jing Zhao, Xijiong Xie, Xin Xu, and Shiliang Sun. 2017. Multi-view learning overview: Recent progress and new challenges. *Information Fusion* 38 (2017), 43–54.

A DEFINITION

A.1 Graph Topological Metrics for CIR

As mentioned Eq. (7) in Section 3, CIR could express many existing topological metrics by adopting different f . Here we list four commonly-used topological metrics in the literature for quantifying Common Interacted Ratio (CIR) between any two nodes i, j . Note that we only consider user-item interactions in our recommendation setting, and hence the common neighborhood set of any pair of user and item would be empty. Thus, we only calculate these metrics for user-user or item-item.

- **Jaccard Similarity (JC) [19]:** The JC score is a classic measure of similarity between two neighborhood sets, which is defined as the ratio of the intersection of two neighborhood sets to the union of these two sets:

$$JC(i, j) = \frac{|\mathcal{N}_i \cap \mathcal{N}_j|}{|\mathcal{N}_i \cup \mathcal{N}_j|} \quad (11)$$

- **Salton Cosine Similarity (SC) [26]:** The SC score measures the cosine similarity between the neighborhood sets of two nodes:

$$SC(i, j) = \frac{|\mathcal{N}_i \cap \mathcal{N}_j|}{\sqrt{|\mathcal{N}_i| \cup |\mathcal{N}_j|}} \quad (12)$$

- **Common Neighbors (CN) [21]:** The CN score measures the number of common neighbors of two nodes and is frequently used for measuring the proximity between two nodes:

$$CN(i, j) = |\mathcal{N}_i \cap \mathcal{N}_j| \quad (13)$$

However, it does not contain any normalization to remove the degree bias in quantifying proximity and hence performs worse than other metrics as demonstrated by our recommendation experiments in Table 3.

- **Leicht-Holme-Nerman (LHN) [17]:** LHN is very similar to SC. However, it removes the square root in the denominator and is more sensitive to the degree of node:

$$LHN(i, j) = \frac{|\mathcal{N}_i \cap \mathcal{N}_j|}{|\mathcal{N}_i| \cdot |\mathcal{N}_j|} \quad (14)$$

We further emphasize that our proposed CIR is a generalized version of these four existing metrics and can be delicately designed towards satisfying downstream tasks. We leave such exploration on the choice of f as one potential future work.

A.2 Subtree and Subgraph Isomorphisms

To demonstrate that our proposed CAGC* can go beyond 1-WL test, we introduce two graph isomorphism concepts as follows:

Definition A.1. Subtree-isomorphism [36]: \mathcal{S}_u and \mathcal{S}_i are subtree-isomorphic [36], denoted as $\mathcal{S}_u \cong_{subtree} \mathcal{S}_i$, if there exists a bijective mapping $h : \tilde{\mathcal{N}}_u^1 \rightarrow \tilde{\mathcal{N}}_i^1$ such that $h(u) = i$ and $\forall v \in \tilde{\mathcal{N}}_u^1, h(v) = j, \mathbf{e}_v^l = \mathbf{e}_j^l$.

Definition A.2. Subgraph-isomorphism [36]: \mathcal{S}_u and \mathcal{S}_i are subgraph-isomorphic [36], denoted as $\mathcal{S}_u \cong_{subgraph} \mathcal{S}_i$, if there exists a bijective mapping $h : \tilde{\mathcal{N}}_u^1 \rightarrow \tilde{\mathcal{N}}_i^1$ such that $h(u) = i$ and $\forall v_1, v_2 \in \tilde{\mathcal{N}}_u^1, e_{v_1 v_2} \in \mathcal{E}_{\mathcal{S}_u}$ iff $e_{h(v_1)h(v_2)} \in \mathcal{E}_{\mathcal{S}_i}$ and $\mathbf{e}_{v_1}^l = \mathbf{e}_{h(v_1)}^l, \mathbf{e}_{v_2}^l = \mathbf{e}_{h(v_2)}^l$.

B THEORETICAL PROOF

This section will thoroughly prove all derivations and theorems in this work. More specifically, Eq. (4) along with Theorem 4.1 and Theorem 4.2.

B.1 Derivation of Eq. (4)

The matrix form of the ranking of user u over item i after L -layer LightGCN-based message-passing is:

$$y_{ui}^L = \left(\sum_{l_1=0}^L \beta_{l_1} \mathbf{E}_u^{l_1} \right)^\top \left(\sum_{l_1=0}^L \beta_{l_1} \mathbf{E}_i^{l_1} \right) = \left(\sum_{l_1=0}^L \beta_{l_1} \tilde{\mathbf{A}}^{l_1} \mathbf{E}^0 \right)_u^\top \left(\sum_{l_1=0}^L \beta_{l_1} \tilde{\mathbf{A}}^{l_1} \mathbf{E}^0 \right)_i \quad (15)$$

Obviously, $\mathbf{E}_u^{l_1} = (\tilde{\mathbf{A}}^{l_1} \mathbf{E}^0)_u = \sum_{j \in \mathcal{P}_u^{l_1, l_1}} \alpha_{ju}^{l_1} \mathbf{e}_j^0$. Therefore, we have:

$$\sum_{l_1=0}^L \beta_{l_1} \mathbf{E}_u^{l_1} = \sum_{l_1=0}^L \beta_{l_1} \sum_{j \in \mathcal{P}_u^{l_1, l_1}} \alpha_{ju}^{l_1} \mathbf{e}_j^0. \quad (16)$$

Eq. (16) means that for each neighborhood layer $\mathcal{N}_u^{l_1}$ ($l_1 \leq L$) around u , for each node $j \in \mathcal{N}_u^{l_1}$, we sum its propagated embedding along the path $P_{ju}^{l_2}$ with the corresponding path coefficient $\alpha_{ju}^{l_2}$ and layer coefficient β_{l_2} over all paths in $\bigcup_{l_3=0}^L \mathcal{P}_{ju}^{l_3}$, i.e., $\forall P_{ju}^{l_2} \in \bigcup_{l_3=0}^L \mathcal{P}_{ju}^{l_3}$, which is equivalent to:

$$\sum_{l_1=0}^L \beta_{l_1} \mathbf{E}_u^{l_1} = \sum_{l_1=0}^L \sum_{j \in \mathcal{N}_u^{l_1}} \sum_{P_{ju}^{l_2} \in \bigcup_{l_3=0}^L \mathcal{P}_{ju}^{l_3}} \beta_{l_2} \alpha_{ju}^{l_2} \mathbf{e}_j^0. \quad (17)$$

Since neighbor $j \in \mathcal{N}_u^{l_1}$ cannot reach u along a path of length less than l_1 and further set $\alpha_{ju}^{l_2} = 0$ if $P_{ju}^{l_2} = \emptyset$, then we have:

$$\sum_{l_1=0}^L \beta_{l_1} \mathbf{E}_u^{l_1} = \sum_{l_1=0}^L \sum_{j \in \mathcal{N}_u^{l_1}} \sum_{l_2=0}^L \beta_{l_2} \alpha_{ju}^{l_2} \mathbf{e}_j^0. \quad (18)$$

Applying the same procedure as above, we can derive the $\sum_{l_1=0}^L \beta_{l_1} \mathbf{E}_i^{l_1}$ and substitute it along with Eq. (18) into Eq. (15), we would end up with Eq. (4).

B.2 Proof of Theorem 4.1

PROOF. We prove this theorem in two directions.

Firstly (\implies), we prove that in a bipartite graph, two subgraphs that are subtree-isomorphic are also subgraph-isomorphic by contradiction. Assuming that there exists two subgraphs $\mathcal{S}_u, \mathcal{S}_i$ that are subtree-isomorphic yet not subgraph-isomorphic in a bipartite graph, i.e., $\mathcal{S}_u \cong_{subtree} \mathcal{S}_i, \mathcal{S}_u \not\cong_{subgraph} \mathcal{S}_i$. By definition of subtree-isomorphism, we trivially have $\mathbf{e}_v^l = \mathbf{e}_{h(v)}^l, \forall v \in \mathcal{V}_{\mathcal{S}_u}$. Then to guarantee $\mathcal{S}_u \not\cong_{subgraph} \mathcal{S}_i$ and also since edges are only allowed to connect u and its neighbors \mathcal{N}_u^1 in the bipartite graph, there must exist at least an edge e_{uv} between u and one of its neighbors $v \in \mathcal{N}_u^1$ such that $e_{uv} \in \mathcal{E}_{\mathcal{S}_u}, e_{h(u)h(v)} \notin \mathcal{E}_{\mathcal{S}_i}$, which contradicts the assumption that $\mathcal{S}_u \cong_{subtree} \mathcal{S}_i$.

Secondly (\impliedby), we can prove that in a bipartite graph, two subgraphs that are subgraph-isomorphic are also subtree-isomorphic, which trivially holds since in any graph, subgraph-isomorphism leads to subtree-isomorphism [36]. \square

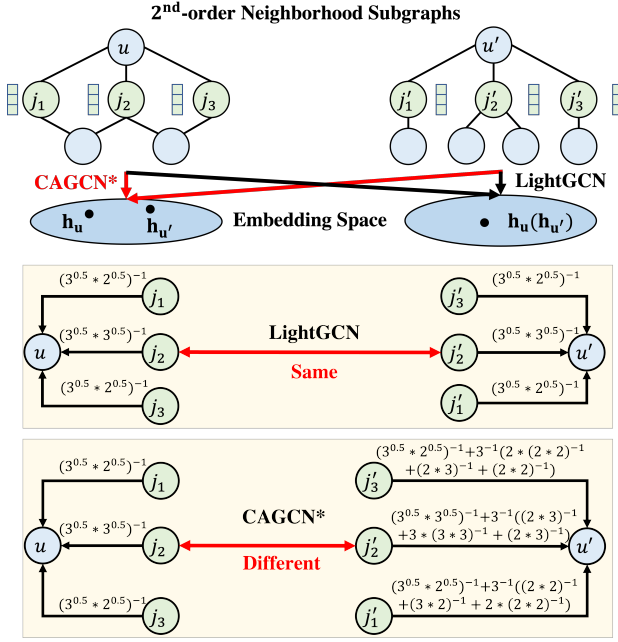


Figure 7: An example showing two neighborhood subgraphs $S_u, S_{u'}$ that are subgraph-isomorphic but not bipartite-subgraph-isomorphic.

B.3 Proof of Theorem 4.2

PROOF. We prove this theorem in two directions.

Firstly (\implies), following [36], we prove that the designed CAGCN* variants satisfy the above two conditions and can distinguish any two graphs that are distinguishable by 1-WL by contradiction. Assume that there exist two graphs \mathcal{G}_1 and \mathcal{G}_2 which can be distinguished by 1-WL but cannot be distinguished by CAGCN*. Further, suppose that 1-WL cannot distinguish these two graphs in the iterations from 0 to $L-1$, but can distinguish them in the L^{th} iteration. Then, there must exist two neighborhood subgraphs S_u and S_i whose neighboring nodes correspond to two different sets of node labels at the L^{th} iteration, i.e., $\{e_v^l | v \in N_u^1\} \neq \{e_j^l | j \in N_i^1\}$. By the condition (2), we know that f is injective. Thus, for S_u and S_i , f would yield two different feature vectors at the L^{th} iteration. This means that CAGCN* can also distinguish \mathcal{G}_1 and \mathcal{G}_2 , which contradicts the assumption.

Secondly (\impliedby), we can prove that there exist at least two graphs that can be distinguished by CAGCN* but cannot be distinguished by 1-WL. Figure 7 presents two of such graphs $S_u, S_{u'}$, which are subgraph isomorphic but non-bipartite-subgraph-isomorphic. Assuming all node embeddings share the same discretization precision and considering u and u' with similar neighborhood feature vectors, then directly propagation according to 1-WL or even considering node degree as the edge weight as GCN [14] can still end up with the same propagated feature for u and u' . Letting g defined in Eq. (10) as weighted summation with $y_i = 1$ and using JC metric to compute ϕ , then we could easily see that propagating according to edge weights computed by CAGCN*-jc would yield different embeddings between u and u' . \square

Table 6: Notations commonly used in this paper and the corresponding descriptions.

Notations	Definitions or Descriptions
$\mathcal{G} = (\mathcal{V}, \mathcal{E})$	Input graph with its node and edge set
\mathcal{U}, \mathcal{I}	User set and item set
m, n	Number of users and items, i.e., $ \mathcal{U} = m, \mathcal{I} = n$
\mathcal{O}	Observed user-item interaction set
$\mathbf{A}, \tilde{\mathbf{A}}$	Adjacency matrix and its normalized version
N_p^l	Set of observed l -hops neighbors of node p
\tilde{N}_p^1	Unobserved 1-hop neighborhood of p
N_p^1	Nodes in N_p^1 including the node p itself
$\tilde{N}_u^1 = \mathcal{V} / (N_u^1 \cup \tilde{N}_u^1)$	In-adjacent nodes of u without u itself
$S_u(\mathcal{S}_i)$	Subgraph induced in \mathcal{G} by $\tilde{N}_u^1(\tilde{N}_i^1)$
\mathcal{P}_{pq}^l	Set of paths of length l between p and q
P_{pq}^l	A specific path of length l between p and q
\mathbf{E}^l	Embeddings of user/item nodes at layer l
d^l	Dimension of embeddings at layer l
y_{ui}	Ranking score of user u over item i
α_{ju}^l	Weight of path of length l from j to u
β_l	Weight of propagation layer l
χ	Collaboration strength
$f(N_i^1, N_j^1)$	Function of j and i 's neighborhood set
Φ	Convolution/Propagation Matrix based on CIR
γ_i	Re-scaling coefficient of node i
g	Function combining propagated embeddings
$\hat{\phi}_u(j) (\phi_u(j))$	(Estimated) Common Interacted Ratio between user u and item j

C MODEL DESCRIPTION

To demonstrate the whole procedure of our CAGCN* shown in Figure 3, we take a specific example of computing the ranking of user u over item i . We first calculate the CIR of each neighbor with respect to the rest of the corresponding neighborhoods as Eq. (10) and then we iteratively propagate neighbors' embeddings with the awareness of the collaboration benefits by following the calculated CIR. Then we weighted combine the propagated embeddings at each layer to obtain the aggregated embedding for u and i . After that, we calculate their ranking based on the dot-product similarity.

D NOTATIONS

Here we summarize notations used throughout the paper in Table 6.

E ADDITIONAL EXPERIMENTAL RESULTS

E.1 Efficiency Comparison

As justified in Section 5.3, the efficiency plays a significant role in evaluating recommendation systems. Following the experimental setting in Figure 4, we present the NDCG@20 with the training time in Figure 8. Clearly, CAGCN* achieves extremely higher performance in significant less time because the collaboration-aware graph convolution leverages more beneficial collaborations from neighborhoods. Similarly to Recall@20 (as seen in Figure 4), we observe the slower performance increase of CAGCN* and LightGCN on ML-1M. We ascribe this to the higher density of ML-1M as in Table 2 that leads to so much noisy neighboring information.

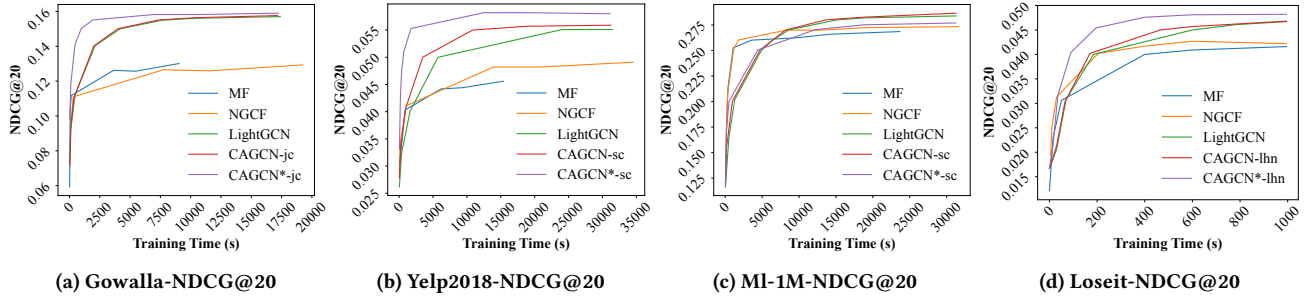


Figure 8: Comparing the training time of CAGCN(*) with other baselines on four datasets. For clear visualization, we only report the efficiency of the best CAGCN(*) variant based on Table 3 for each dataset. CAGCN* almost always achieves extremely higher NDCG@20 with significant less time.

One future direction could be to leverage the CIR to prune the graph of these noisy connections in an iterative fashion as either a preprocessing step or even used throughout training when paired with an attention mechanism (although the latter would come at significantly longer training time).

E.2 Performance Interpretation

To demonstrate the generality of our observation in Figure 6, we further perform exactly the same analysis on Yelp (shown in Figure 9) and derive almost the same insights: 1) Graph-based recommendation models achieve higher performance than non-graph-based ones for lower degree nodes; 2) the opposite performance trends between NDCG and Recall indicates that different evaluation metrics have different levels of sensitivity to node degrees.

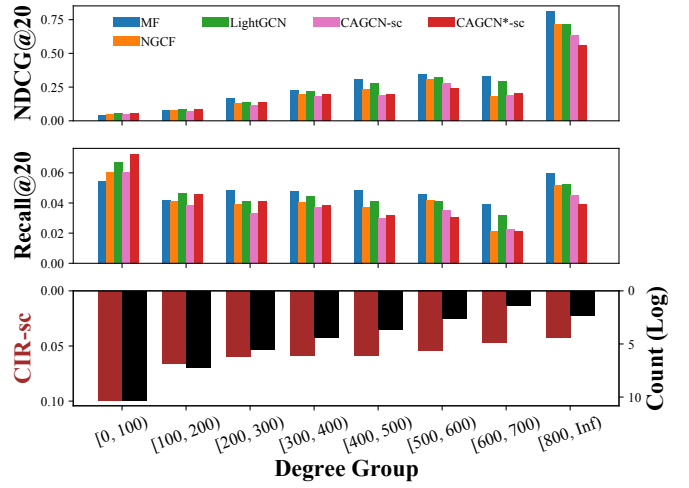


Figure 9: The performance of each model w.r.t. node degree on Yelp.